JOURNAL OF MATERIALS SCIENCE 25 (1990) 3709-3713

Phase transformation and densification during pressureless sintering of Si_3N_4 with MgO and $Y_3Al_5O_{12}$ additives

M. PROKEŠOVÁ, Z. PÁNEK
Institute of Inorganic Chemistry, Centre for Chemical Research, Slovak Academy of Sciences, Dúbravská cesta 9, CS-842 36 Bratislava, Czechoslovakia

The α–β transformation of Si_3N_4 during liquid-phase sintering appears to be controlled by the growth of the β-Si_3N_4 grains in the direction perpendicular to the c-axis in the case of MgO additive. The diffusion through the liquid is the rate-controlling step in the case of the $Y_3Al_5O_{12}$ additive. The density of the sintered body at the solid skeleton stage was influenced by the change in the α–β transformation rate and/or by a change of the transformation mechanism. The indirect proportionality between the β-phase content in the starting powder and the density at the solid skeleton stage was found. The microstructure of the sintered body is influenced by both the β-phase content in the starting powder and the chemical composition of the additive. Fine, uniform microstructure with a high aspect ratio of β-grains is obtained, when the β-phase content in the starting powder is as small as possible and when the α–β transformation is controlled by grain growth.

1. Introduction

The microstructure and physico-chemical properties of sintered Si_3N_4 materials depend on the physical, chemical and crystallographic characteristics of Si_3N_4 starting powders, the chemical composition and the amount of additive forming the liquid at the sintering temperature and on the processing parameters [1–4]. Generally, fine, uniform microstructures with a high aspect ratio of β-grains lead to good mechanical properties of Si_3N_4 products [3–5].

If the starting powder contains a large amount of the thermodynamically stable polydisperse β-Si_3N_4 phase, dissolved fine β-particles will continuously be reprecipitated on the coarser original β-particles under nearly equilibrium conditions [2]. The resulting microstructure will consist of the large equiaxed β-grains.

On the other hand, if the content of β-phase in the starting powder is low, the supersaturation of the liquid has to be caused locally due to the lack of primary β-particles. This leads to the spontaneous nucleation and the crystallization of idiomorphic rod-like β-grains, far from the thermodynamic equilibrium [2]. Resulting microstructure consists of the rod-like β-grains [1–3].

The green body densification during liquid-phase sintering (LPS) is based on the rearrangement and the shape changes of the starting solid constituents. The LPS is conventionally divided into three stages: particle rearrangement, solution–diffusion–reprecipitation and solid skeleton sintering [6–8]. A schematic description of the possible densification mechanism of Si_3N_4 during the α–β transformation is given by Weiss and Kaysser [7]. This model assumes that solution–diffusion–reprecipitation starts when the primary rearrangement (i.e. rearrangement, which is controlled by mechanical movement due to the capillary forces) is finished, but really these two stages are simultaneous [9]. When the rod-like β-grains impinged each other (the solid skeleton stage), the densification stopped.

It seems reasonable to consider that the initial dissolution of Si_3N_4 from the areas of highest curvature promotes particle rearrangement, but subsequent reprecipitation of the rod-like β-grains will have the opposite effect [10].

In the present work, an attempt is made to evaluate the influence of α–β transformation on the formation of microstructures of silicon nitride ceramics during LPS.

2. Experimental procedure

The starting silicon nitride powder used in this study was prepared by the carbothermal reduction and nitridation of SiO_2 [11]. The particle size and morphology of starting powder A is illustrated in Fig. 1.

TABLE I Properties of starting Si_3N_4 powders

Powder type	A	B
Specific surface area ($m^2 g^{-1}$) (BET)	9	9
O* (wt %)	3.5	3.3
C (wt %) (LECO)	0.9	0.8
$\alpha/(\alpha + \beta)$ (wt %) (XRD)	98	90
Morphology	equiaxed	equiaxed

*By neutron activation analysis.

0022-2461/90 $03.00 + .12 © *1990 Chapman and Hall Ltd.*

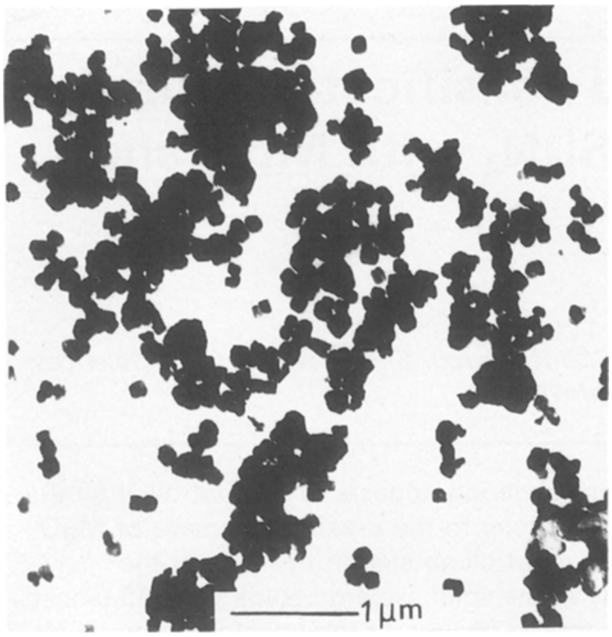

Figure 1 Transmission electron micrograph of starting Si_3N_4 powder A.

Powder B was prepared from powder A by the addition of the fine Si_3N_4 powder ($d \leqslant 0.5\,\mu m$), whose β-phase content was about 50 wt %. The fine Si_3N_4 powder was obtained from SPS powder (Soviet Provenance) after centrifugation of the non-sedimenting suspension of this powder in dry acetone. The characteristics of powders A and B were determined and the results are summarized in Table I.

Two types of the liquid-phase forming additives were used: MgO and a mixture of Y_2O_3 with Al_2O_3 in the molar ratio corresponding to the yttrium–aluminium garnet (YAG). MgO was added in the form of $Mg(NO_3)_2$ to the Si_3N_4 powder. The mixture was homogenized in ethanol, then dried and subsequently decomposed at 500° C. Y_2O_3 and Al_2O_3 were added in the form of water solution of $Y(NO_3)_3$ and $Al(NO_3)_3$ to the water suspension of Si_3N_4. An appropriate amount of urea was added for the co-precipitation of $Y(OH)_3$ and $Al(OH)_3$. This suspension was heated at 100° C for 1 h, then filtered, dried, decomposed at 500° C and homogenized in ethanol.

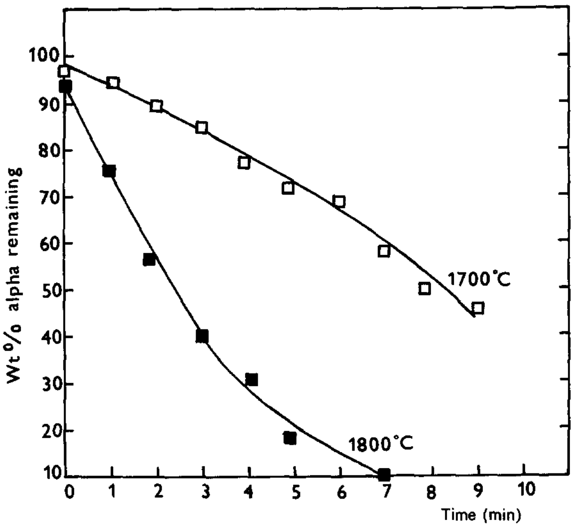

Figure 3 Time-dependence of α–β conversion for Si_3N_4–10 wt % YAG at (□) 1700 and (■) 1800° C (AG).

The powder mixtures containing 5 wt % MgO (AM, BM for powders A and B, respectively) and 10 wt % YAG (AG, BG) were pressed in a steel die under a pressure of 100 MPa. Finally, the powder compacts were pressed by cold isostatic pressing at a pressure of 200 MPa. The green densities of compacts prepared in this way were approximately 46% theoretical for both the YAG and MgO additives. These powder compacts were isothermally sintered in a graphite resistance-heated furnace under 1 MPa nitrogen at 1700 and 1800° C for 0 to 10 min. Each compact was embedded in a powder bed, which was a mixture of BN and powder of the same composition as the green compact. The function of the powder bed was described by Mangels [12].

Both the green and final densities of every compact were calculated from its mass and dimensions; the density of the sintered compact was also measured by mercury displacement. The measured and calculated densities of the sintered compact were found to be in very good agreement. The weight loss of each compact was determined after sintering. The content of α-Si_3N_4

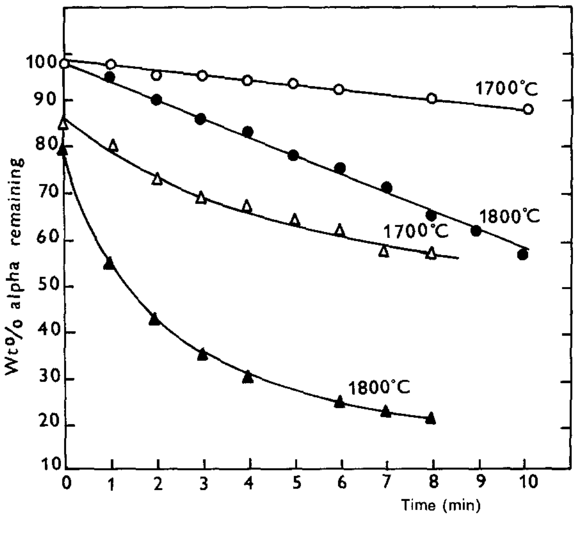

Figure 2 Time-dependence of α–β conversion for Si_3N_4–5 wt % MgO at 1700 and 1800° C: (○, ●) AM; (△, ▲) BM.

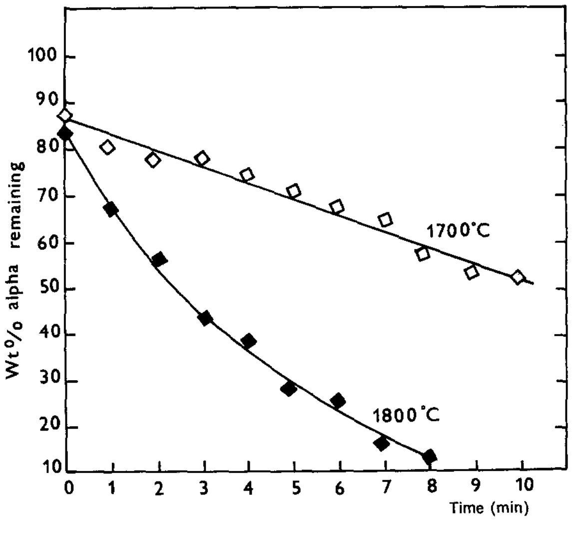

Figure 4 Time-dependence of α–β conversion for Si_3N_4–10 wt % YAG at (◇) 1700 and (◆) 1800° C (BG).

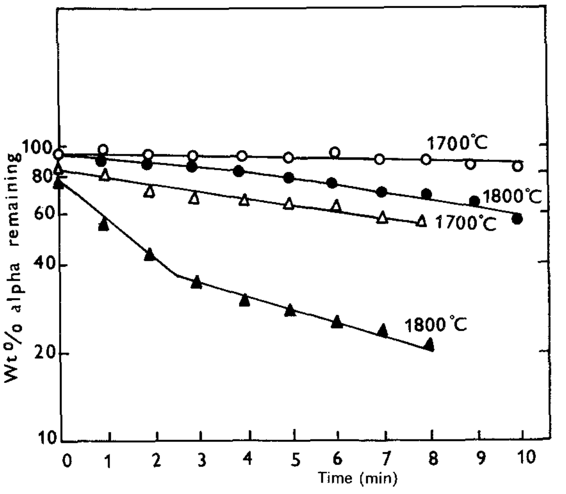

Figure 5 Time-dependence of $\log_{10}\alpha$ for Si_3N_4–5 wt % MgO at 1700 and 1800° C. (○, ●) AM, (△, ▲) BM.

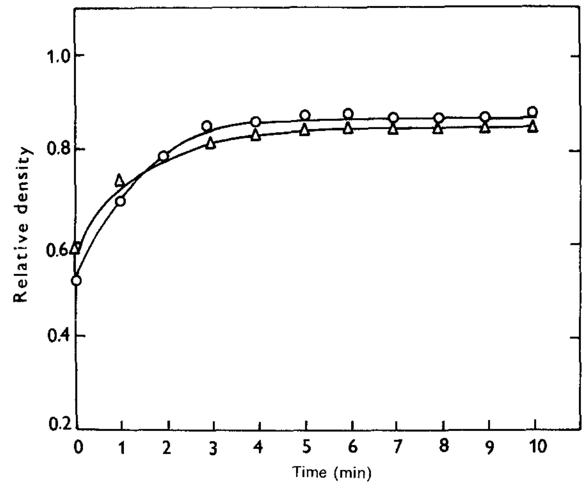

Figure 7 Densification data for Si_3N_4–5 wt % MgO at 1700° C. (○) AM, (△) BM.

was calculated from the ratio of XRD intensities of $[2\,1\,0]_\alpha$ and $[2\,1\,0]_\beta$ planes [13]. The microstructure was investigated from scanning electron micrographs.

3. Results and discussion

3.1. Kinetics of phase transformation

The time dependence of the α–β transformation for samples AM, BM, AG and BG at a given temperature is shown in Figs. 2 to 4. These curves suggest the first-order conversion kinetics described by the equation

$$\frac{d\alpha}{dt} = -K\alpha \qquad (1)$$

where K is the rate constant and α is the content of α phase in the sintered sample. The plots of log α against time are linear, which supports the validity of Equation 1 (Figs 5, 6). The time dependences of log α in some cases (sample BM at 1800° C in Fig. 5 all samples in Fig. 6) consist of two straight lines, which suggest a change of the rate constant in these cases.

3.2. Si_3N_4–MgO system

Three rate-limiting mechanisms are suggested during the early stage of α–β transformation: dissolution of the α-phase in the liquid, diffusion through the liquid and reprecipitation of β-phase [14]. Knoch and Gazza [14] supposed that the diffusion distances were short and the diffusion through the liquid phase was fast; therefore, the diffusion as the rate-limiting mechanism can be excluded. An increase in the conversion rate with increasing β-phase content in the starting powder (Fig. 5) suggests that the α–β transformation is controlled by the α/liquid/β interface area and the growth of β-phase on the pre-existing β-grains is dominant. The different growth rates in parallel and perpendicular directions to the c-axis result in rod-like β-grains. It can be concluded, that the rate-limiting mechanism is the growth of β-grains perpendicular to the c-axis.

The time dependence of densification for the samples AM and BM at given temperatures are given in Figs 7 and 8. As conversion rate increases the maximum density reached decreases. The value of maximum density reached is limited by the density level at the time of transition to the solid skeleton sintering, when the further α–β transformation continues without significant contribution to the densification [15, 16]. The solid skeleton stage was observed at the essentially lower value of β-phase content in the sintered sample AM (15 wt % after 4 min at 1800° C) as in sample BM (60 wt % after 2 to 3 min at 1800° C, Figs 5 and 8). This can be explained as follows: (1) if the starting powder contains only a small number of

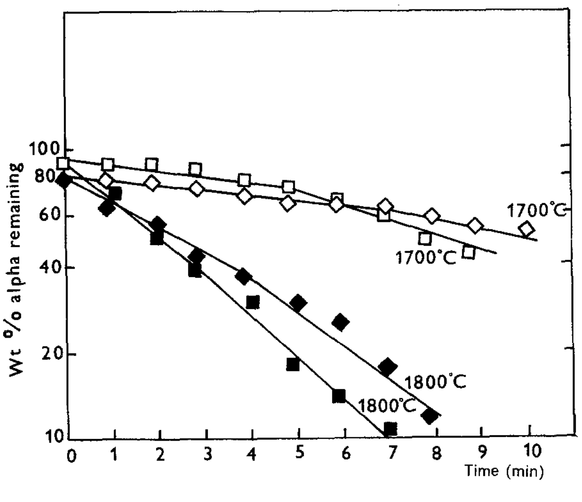

Figure 6 Time-dependence of $\log_{10}\alpha$ for Si_3N_4–10 wt % YAG at 1700 and 1800° C. (□, ■) AG, (◇, ◆) BG.

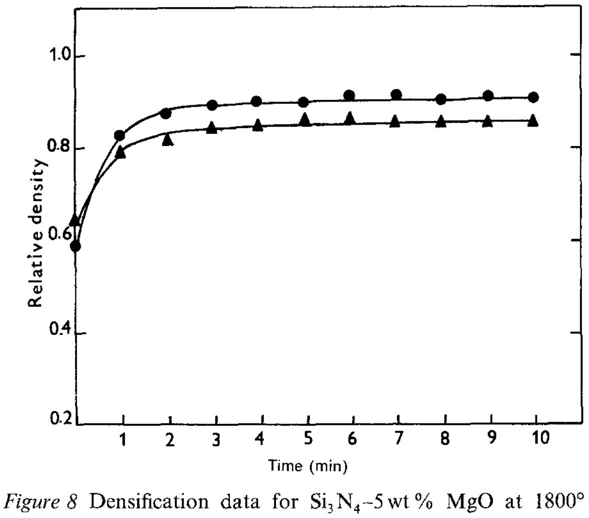

Figure 8 Densification data for Si_3N_4–5 wt % MgO at 1800° C. (●) AM, (▲) BM.

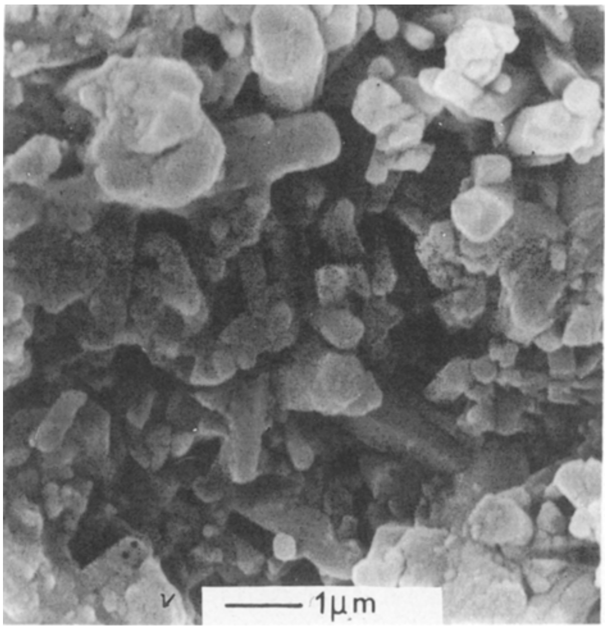

Figure 9 Scanning electron micrograph of the fracture surface of Si_3N_4–5 wt % MgO specimen (AM) sintered at 1800° C for 7 min.

β-grains, a high supersaturation in the liquid phase must be created due to the lack of β-nuclei; (2) if the starting powder contains a sufficient number of β-grains, which can be considered as pre-existing β-nuclei, such supersaturation is not necessary for crystallization. In the first case a higher amount of α-phase is dissolved in the liquid prior to the initiation of the α–β conversion. Hence, a higher value of density is reached by the primary rearrangement. In the second case an increase of the initial α–β conversion rate causes a decrease in mobility of reprecipitated rod-like β-grains. An increase in density due to the primary rearrangement is therefore lower compared to the first case. The rate constant of α–β conversion is changed in the solid skeleton stage (see Fig. 5), probably due to a reduction of the α/β interface and/or by a depletion of α-phase in some areas.

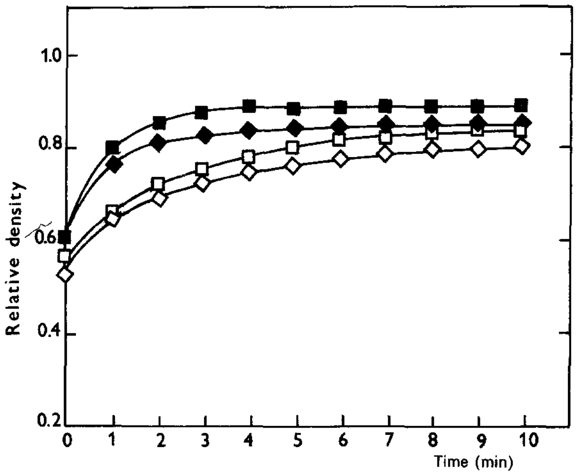

Figure 11 Densification data for Si_3N_4–10 wt % YAG at (□, ◇) 1700 and (■, ◆) 1800° C. (□, ■) AG, (◇, ◆) BG.

Figs 9 and 10 show the microstructure of sintered samples AM and BM. Comparing these microstructures, it may be concluded that sample AM has a finer and a more rod-like microstructure. It can be assumed that if a high number of growing grains is present (BM), less total growth per grain is necessary to obtain the same volume fraction of β-phase. It also means, that resulting microstructure is less rod-like (Fig. 10).

3.3. Si_3N_4–YAG system

An increase of initial β-phase content results in a slight decrease of the rate constant, *K* (Fig. 6). The total decrease of conversion rate in sample BG and the points of intersection of curves in Fig. 6 can be explained on the basis of "nucleation inactivity" of the pre-existing β-grains. This inactivity is probably a consequence of very large distances between the β-grains and low diffusivities in the liquid. Therefore, in both cases (AG, BG) local supersaturation in the liquid can be created, which results in spontaneous nucleation and crystallization of rod-like grains rather than growth of pre-existing β-grains. Thus α–β transformation must be controlled by the diffusion.

The content of preferentially soluble α-phase is

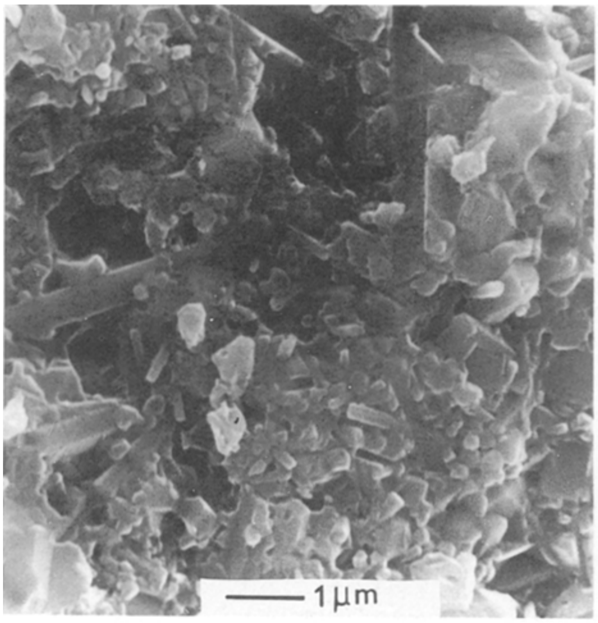

Figure 10 Scanning electron micrograph of the fracture surface of Si_3N_4–5 wt % MgO specimen (BM) sintered at 1800° C for 7 min.

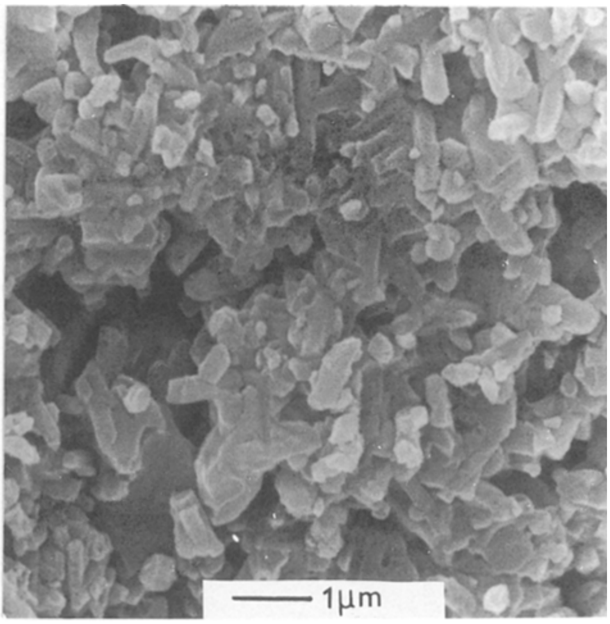

Figure 12 Scanning electron micrograph of the fracture surface of Si_3N_4–10 wt % YAG specimen (AG) sintered at 1800° C for 7 min.

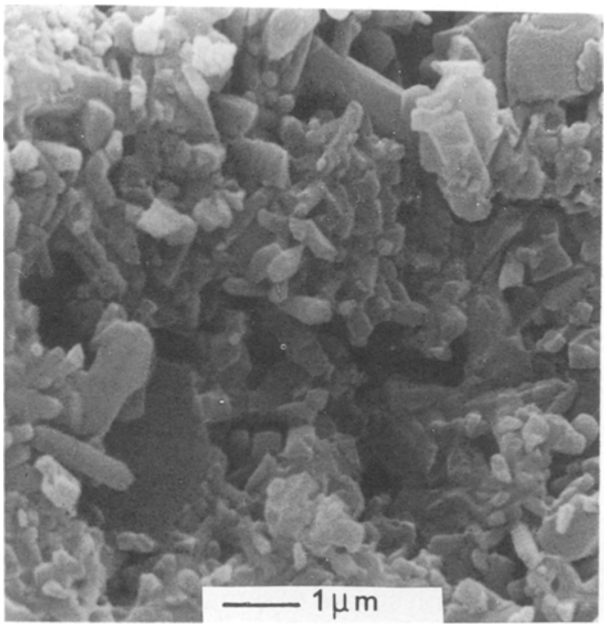

Figure 13 Scanning electron micrograph of the fracture surface of Si_3N_4–10 wt % YAG specimen (BG) sintered at 1800° C for 7 min.

decreased if the β-phase content in the starting powder has been increased. The local supersaturation is then reached after a longer time period. The resulting effect is the decrease of the rate constant, K.

The time dependences of densification for samples AG, BG are in Fig. 11. The solid skeleton stage was observed at the same β-phase content (about 60 wt %) for both samples AG, BG (see Figs 6, 11) at 1800° C and also the microstructures were similar (Figs 12, 13). The density at this transition stage is indirectly proportional to the β-phase content in starting powder. This behaviour can be explained by more effective particle rearrangement during the early stage of LPS in the composition containing higher a content of preferentially soluble α-phase (samples AG).

4. Conclusions

For MgO additive:

1. The reconstructive α–β transformation during LPS of Si_3N_4 appears to be controlled by the chemical reaction; the growth of β-grains is the rate-controlling step.

2. A direct proportionality between the starting β-phase content and the transformation rate was found.

3. A change in transformation rate at the solid skeleton stage was observed, further α–β transformation continues without a significant contribution to the densification.

For YAG additive:

4. The α–β transformation appears to be controlled by the diffusion.

5. An indirect proportionality between the starting β-phase content and transformation rate was found.

For both additives:

6. An indirect proportionality between the β-phase content in the starting powder and the density at the solid skeleton stage was found.

7. The microstructure of the sintered body is influenced by the β-phase content in the starting powder, as well as by the chemical composition of the additive.

8. To obtain fine, uniform microstructure with a high aspect ratio of β-grains, a β-phase content as small as possible in the starting powder and control of the α–β transformation by grain growth are necessary.

References

1. B. WÖTTING, B. KANKA and G. ZIEGLER, "Non-oxide Technical and Engineering Ceramics", edited by Stuart Hampshire (Elsevier Applied Science, London, 1986) p. 83.
2. G. ZIEGLER, J. HEINRICH and B. WÖTTING, *J. Mater. Sci.* **22** (1987) 3041.
3. F. F. LANGE, *J. Amer. Ceram. Soc.* **62** (1979) 428.
4. G. WÖTTING and G. ZIEGLER, *Ceram. Int.* **10** (1984) 18.
5. G. HIMSOLT *et al.*, *J. Amer. Ceram. Soc.* **62** (1979) 21.
6. W. D. KINGERY, *J. Appl. Phys.* **30** (1959) 301.
7. J. WEISS and W. A. KAYSSER, in "Progress in Nitrogen Ceramics", edited by F. L. Riley (Martinus-Nijhoff, Boston, The Hague, Dordrecht, Lancaster, 1983) p. 169.
8. G. PETZOW and A. KAYSSER, in "Sintered Metal-Ceramic Composites", edited by G. S. Upadhyaya (Elsevier, Amsterdam, 1984) p. 51.
9. L. J. BOWEN *et al.*, *J. Mater. Sci.* **13** (1978) 341.
10. M. PROKEŠOVÁ and Z. PÁNEK, *Ceram. Int.* **15** (1989) 369.
11. V. FIGUSCH and T. LIČKO, in "High Tech Ceramics", edited by P. Vincenzini (Elsevier, Amsterdam, 1987) p. 517.
12. J. A. MANGELS, in "Progress in Nitrogen Ceramics", edited by F. L. Riley (Martinus-Nijhoff, Boston, The Hague, Dordrecht, Lancaster, 1983) p. 231.
13. C. P. GAZZARA and D. R. MESSIER, *Amer. Ceram. Soc. Bull.* **56** (1977) 777.
14. H. KNOCH and G. E. GAZZA, *Ceram. Int.* **6** (1980) 51.
15. G. PETZOW and W. J. HUPPMANN, *Z. Metallkde* **67** (1976) 579.
16. W. J. HUPPMANN, *ibid.* **70** (1979) H12.

Received 6 April
and accepted 28 September 1989